

# Strengthening of semicoke based carbon composites through multi-wall carbon nanotubes

Rajeev Kumar · Sanjay R. Dhakate ·  
R. B. Mathur

Received: 22 April 2013 / Accepted: 18 May 2013 / Published online: 7 June 2013  
© The Author(s) 2013. This article is published with open access at Springerlink.com

**Abstract** The present investigation explored the possibility of developing carbon composites using semicoke as matrix precursor and multi-walled carbon nanotubes (MWCNTs) as reinforcement. The different weight fraction of MWCNTs was incorporated in semicoke-based composites, and these composites were heat treated at 1,000, 1,400 and 2,500 °C. The MWCNTs carbon composite was characterized for electrical, thermal and mechanical properties. It was observed that the bulk density of composites with 1 wt% of MWCNTs was 1.92 g/cc, whereas without nanotubes it was 1.87 g/cc. The bending strength of carbonized composites was increased by 78 % and that of graphitized ones by 69 % at 1 wt% of MWCNTs. This value of bending strength was three times higher than that of conventional graphite. The electrical and thermal conductivity increased by 12 and 33 %, respectively. The Raman spectroscopic studies showed that intensity ratio of D and G band (ID)/(IG) ratio minimum deflects the lower level of defects and higher degree of graphitization in carbon composites at 1 wt% of MWCNTs. This demonstrates that in case of MWCNTs, semicoke-based carbon composites with 1 wt% of MWCNTs were sufficient for strengthening carbon composites, if MWCNTs were well dispersed in semicoke.

**Keywords** Coal tar pitch · Semi coke · MWCNTs · Electrical · Thermal and mechanical properties · Composite

## Introduction

Carbon–Carbon (C–C) composites are an important class of ceramic materials that have many potential applications due to their unique thermal, electrical and mechanical properties. In inert atmosphere, C–C composites can retain their properties to temperature  $\sim 3,000$  °C (Fitzer 1987; Mantell 1968). They are used in many advanced technologies in different fields, such as brake pads for both civilian and military aircraft, rocket nozzles, battery electrodes, thermal management, seal and friction materials, etc. (Schmidt et al. 1998; Blanco et al. 2000). However, the conventional techniques of preparing C–C composites are complicated, expensive and time-consuming, such as liquid phase impregnation and chemical vapour deposition, which are indispensable for obtaining high-performance C–C composite materials (Aly-Hasan et al. 2003). In these techniques, carbon matrices are derived from either pitches, polymeric resin, or chemical vapour infiltration (Li 2001); both processes take long fabrication time and have high production costs. Impregnation/carbonization with pitch or resin needs a number of cycles to attain high-density C–C composite because of the low carbon yield. Although high-pressure carbonization process improves carbon yield and decreases fabrication cycles, it requires expensive equipment which results in high costs. Much effort has been undertaken to develop C–C composites by new methods to simplify the processing and hence, reduce time. The mesophase pitch has high carbon yield and it gives graphitizable carbon, which is recognized as an excellent precursor for high-performance C–C composite and graphite (Thomas 1993; Song et al. 2004; Wang et al. 1999; Bhatia et al. 1994). Many researchers have explored mesocarbon microbeads (MCMB) as an excellent precursor for development of high-density carbon and C–C

R. Kumar · S. R. Dhakate (✉) · R. B. Mathur  
Physics and Engineering of Carbon, Division of Materials  
Physics and Engineering, CSIR-National Physical Laboratory,  
New Delhi 110012, India  
e-mail: dhakate@mail.nplindia.org

composite materials (Wang et al. 1999; Gao et al. 2002). On the other hand, due to the extraordinary properties of nanomaterial, it has tremendous potential to improve the properties of C–C composites by incorporating few weight percentages. Since the discovery of carbon nanotubes (CNTs) by Ijima 1991, there is lot of work worldwide carried on CNTs-based composites owing to their unique electrical, thermal and mechanical properties. The CNTs are thought to be the ultimate in carbon fibres having ultra-high thermal conductivity, and high mechanical and unusual electrical properties (Dresselhaus and Avouris 2001; Yu et al. 2000a, b; Ajayan et al. 1994). Even in composites a very small amount of CNTs can induce significant changes in the material's properties. At present much work continues on the development of CNTs reinforced polymer, ceramic and metal matrix composites (Peigney et al. 2000; Ning et al. 2003; Qiu et al. 2003). However, very little work is carried out on carbon-reinforced carbon composites (Gao et al. 2005; Song et al. 2007; Song et al. 2008). Gao et al. 2005 developed a MWCNTs-reinforced carbon matrix composite in which the mesophase pitch is used as the carbon matrix with different contents of MWCNTs. It is reported that, carbon composites flexural strength is 67 MPa and electrical resistivity 17.84  $\mu\Omega$  m for 20 wt% MWCNTs, thermal conductivity 78 W/m K for 5 wt% MWCNTs in composite heat treated at 2,500 °C for 1 h. Song et al. 2007, fabricated the carbon composites from the oxidized mesophase pitch and MWCNTs, with varying MWCNTs content from 5 to 20 wt%. It is reported that flexural strength increases from 60.5 to 78.6 MPa, electrical conductivity from 854 to 1175 S/cm, and thermal conductivity 53.6–118 W/m K of carbon composites with addition 5 wt% of MWCNTs. Song et al. 2008 prepared the carbon composites with matrix derived from mesocarbon microbeads and surface-treated MWCNTs in different weight contents (from 5 to 20 wt%) as reinforcement. The maximum flexural strength (63 MPa), electrical conductivity (596 S/cm) and thermal conductivity (65.8 W/m K) are achieved at 10 wt% of MWCNTs in composites.

In the present investigation, MWCNTs-based carbon composites is developed using coal tar pitch-based semicoke as the matrix precursor and MWCNTs as the reinforcement. The semicoke is low volatile intermediate product between pitch and coke, due to its low volatile product content and  $\beta$ -resin, which is responsible for interaction with reinforcement. It can yield high-density composites with improved properties. The composites are heat treated at 1,000, 1,400 and 2,500 °C in inert atmosphere. To ascertain the effect of MWCNTs and processing parameters on the carbon composites, the composites are characterized for electrical thermal and mechanical properties.

## Experimental and characterization

### Raw materials and preparation of CNT-carbon composites

Coal tar pitch was used as starting material procured from M/s Konark Tar Products. The coal tar pitch possesses softening point 86.6 °C, quinoline insoluble (Q.I.) content 0.3 %, toluene insoluble (T.I.) content 15.9 % and a coking value of 47.6 %. The coal tar pitch was heat treated at 480 °C for 4 h in nitrogen atmosphere to obtain the self-sintering carbonaceous material called semicoke. This semicoke was grounded by centrifugal ball mill to get a fine powder. This semicoke powder possesses Q.I. content 94.7 %, T.I. content 97.8 %, coking value 90.7 % and volatile matter content of 9.3 %. The block of semicoke of size 45 mm  $\times$  15 mm  $\times$  5 mm was moulded at room temperature by compression-moulding technique. In another set of experiments MWCNTs-incorporated semicoke blocks were prepared. The MWCNTs-based carbon composites were prepared by using commercial MWCNTs (Nanocyl, Belgium) in different weight fractions (1–10 wt%). The MWCNTs initially dispersed in organic solvent (acetone) by ultra-sonication and magnetic stirring. The dispersed nanotubes were mixed with semicoke through ball milling. The mixture later on was moulded into blocks/plates by compression-moulding technique at room temperature. All blocks were carbonized at 1,000, 1,400 °C and graphitized at 2,500 °C in inert atmosphere to obtain the high-density graphite blocks and MWCNTs-based carbon composites.

### Characterization of raw material and composites

Fourier Transform Infra-Red (FT-IR) spectroscopy was used to characterize coal tar pitch, semicoke and MWCNTs using FT-IR spectrometer Thermo Nicolet model 380 having resolution of 4  $\text{cm}^{-1}$  in transmittance mode in the spectral range 4,000–400 wave number ( $\text{cm}^{-1}$ ).

The X-ray photoelectron spectroscopy (XPS) spectra of the MWCNTs and semicoke were obtained using a MultiLab 2000 spectrometer (Thermo Electron Corporation, England) to investigate the elements' composition and surface groups present on the surface of the samples. Al Ka (1,485.6 eV) was used as the X-ray source with a 14.9 keV anode voltage, a 4.6 A filament current and a 20 mA emission current. The XPS survey spectra were obtained with 50-eV pass energy and a 0.5-eV step size. Core level spectra were obtained at 20-eV pass energy with a 0.05-eV step size. To get the quantitative analysis of surface complex available on the MWCNTs and semicoke, both were characterized by thermogravimetric analyzer (TGA, Mettler Toledo 851) in nitrogen atmosphere up to 1,000 °C at

10 °C/min. The surface morphology of the few samples was observed by using a scanning electron microscope (SEM) LEO-440 and ZEISS-EVO MA10. The thermal conductivity of carbon composites was measured by laser flash method having xenon laser as the source in thermo flash line 2003 instrument (Anter Corporation, USA). The test sample of size 12.7 mm × 12.7 mm × 3 mm was used and test performed in vacuum environment by the laser flash method. The thermal diffusivity and specific heat of each sample were measured at 25 °C. The thermal conductivity was calculated from the equation,  $\alpha = k/\rho.Cp$ ,

where  $\alpha$  is the thermal diffusivity,  $k$  is the thermal conductivity,  $Cp$  is the specific heat and  $\rho$  is the density of the composite.

The electrical conductivity of composites was measured by using a four-probe technique. A Keithley 224 programmable current source was used for providing constant current ( $I$ ). The voltage drop ( $V$ ) in between two pinpoints with a span of 1.2 cm was measured by Keithley 197 A auto ranging microvolt DMM.

Raman spectra of MWCNTs and carbon composites were recorded using Renishaw Raman Spectrometer, Germany, with laser as excitation source at 514 nm. All spectra were recorded under the same experimental conditions. The crystal structure of carbon composites graphitized at 2,500 °C was determined by analyzing the powdered specimen by X-ray diffraction (XRD) technique employing D-8 Advanced Bruker powder X-ray diffractometer using  $\text{CuK}_\alpha$  radiation ( $\lambda = 1.5418 \text{ \AA}$ ) spectrometer. The MWCNTs-incorporated carbon composites bending strength was measured by a three-point bending technique on Instron Universal Testing Machine model 4411 as per ASTM standard.

## Results and discussion

### XPS of MWCNTs and semicoke

The XPS spectra of MWCNTs and semicoke are illustrated in Figs. 1 and 2. Any reinforcing or matrix material used in the development of composites possesses functional groups on their surface. These groups generally are responsible for interaction or bonding between reinforcing and the matrix phase. The XPS is an excellent tool to identify the functional groups present on the surface in the quantitative amount. Figure 1a, b shows the deconvolution of XPS spectra of MWCNTs for carbon and oxygen. The C1s and O1s spectra involve the electron transition from carbon-oxygen atoms of different atomic configurations, and their shape depends upon atomic densities. The evaluation of bonding content consists of spectra background subtraction, followed by fitting of Gaussian-Lorentzian

asymmetric functions to the measured spectra, selecting the relevant binding energy values from literature (Song et al. 2008; Titantah and Lamoen 2005). In both the cases, asymmetric peaks are observed centred at different binding energies with long tail extended to the higher energy region. The deconvolution of C1s spectra is split into four peaks, C1s A of carbon in graphitic type, C1s B of carbon singly bound to oxygen (C–O) in phenols and ethers, C1s C of carbon doubly bound to oxygen (C=O) in ketones and quinones, C1s D of carbon bound to two oxygen (–COO) in carboxyl, carboxylic anhydrides and ester. The deconvolution of the O1s spectrum results in three peaks (Fig. 1b), oxygen doubly bound to carbon (O=C) in the form of quinones, ketones and aldehydes and oxygen single bound to carbon (O–C) in the form of ethers and phenols. Figure 2 shows the deconvolution XPS spectra (C1s and O1s) of semicoke derived from coal tar pitch. The deconvolution of C1s spectra is split into four peaks (Fig. 2a), C1s A of carbon in graphitic type, C1s B of carbon singly bound to oxygen (C–O) in phenols and ethers, C1s C of carbon doubly bound to oxygen (C=O) in ketones and quinones, C1s D of carbon bound to two oxygen (–COO) in carboxyl, carboxylic anhydrides and ester. The deconvolution of the O1s spectrum results in three peaks (Fig. 2b), oxygen doubly bound to carbon (O=C) in the form of quinones, ketones and aldehydes and oxygen single bound to carbon (O–C) in the form of ethers and phenols.

Table 1 compares the binding energies and atomic percentage of different functional groups attached with surfaces of MWCNTs and semicoke particles. In the case of MWCNTs, peaks observed at 285.02, 286.49, 288.23, 291 eV in C1s spectra correspond to graphitic C, alcohol or ether, carbonyl and carboxylic groups or  $\pi$ – $\pi$  transition of aromatic ring. But slight change in the binding energy <0.35 eV is considered insignificant based on the energy resolution of the XPS instrument used. On the other hand, in O1s A spectra, peak at 530.69 eV and O1s B corresponds to C=O and C–O. But, O1s C spectra, peak at 535.15 eV corresponds to the water molecule due to the absorption of moisture by nanotubes or due to carbonyl group. In case of semi-coke, peaks observed at 284.9, 286.5, 288.2, 290 eV is of C1s spectra correspond to graphitic and non-graphitic carbon, phenyl and ether, carbonyl and carboxylic groups, respectively. On the other hand, in oxygen spectra, spectra O1s A peak at 532.64, O1s B at 530.5 and O1s C at 534.897 eV corresponds to C–O, C=O, –COO, respectively.

### FT-IR studies of MWCNTs and semicoke

Coal tar pitch is complex material containing hundreds of compounds with different functionalities. Therefore, coal

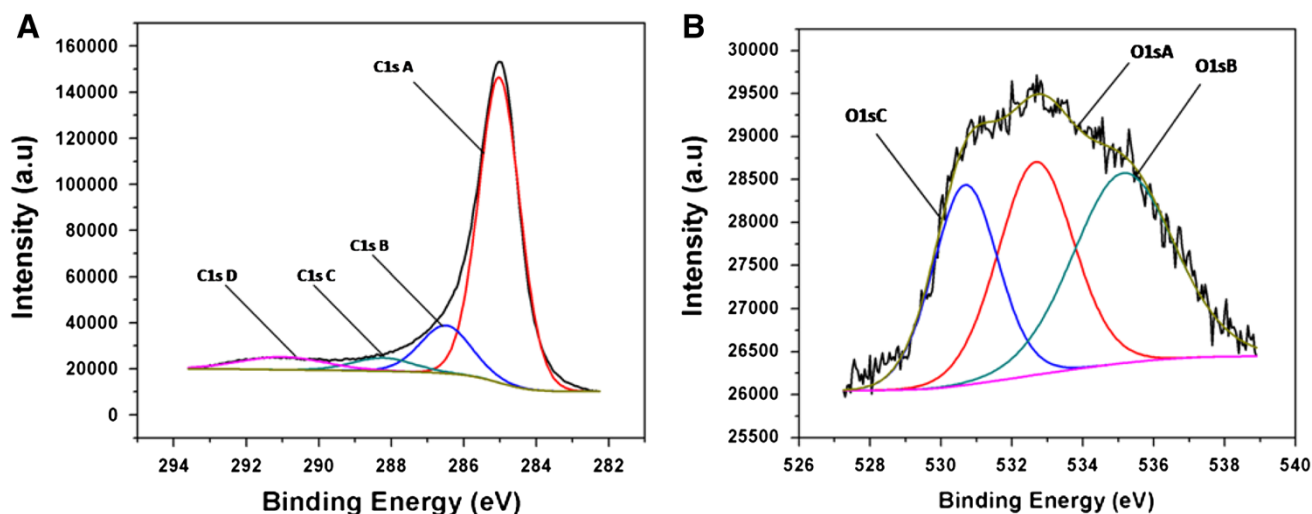


**Fig. 1** X-ray Photoelectron Spectroscopy spectra of MWCNTs (a) deconvoluted spectra of C1s region and (b) deconvoluted spectra of O1s region

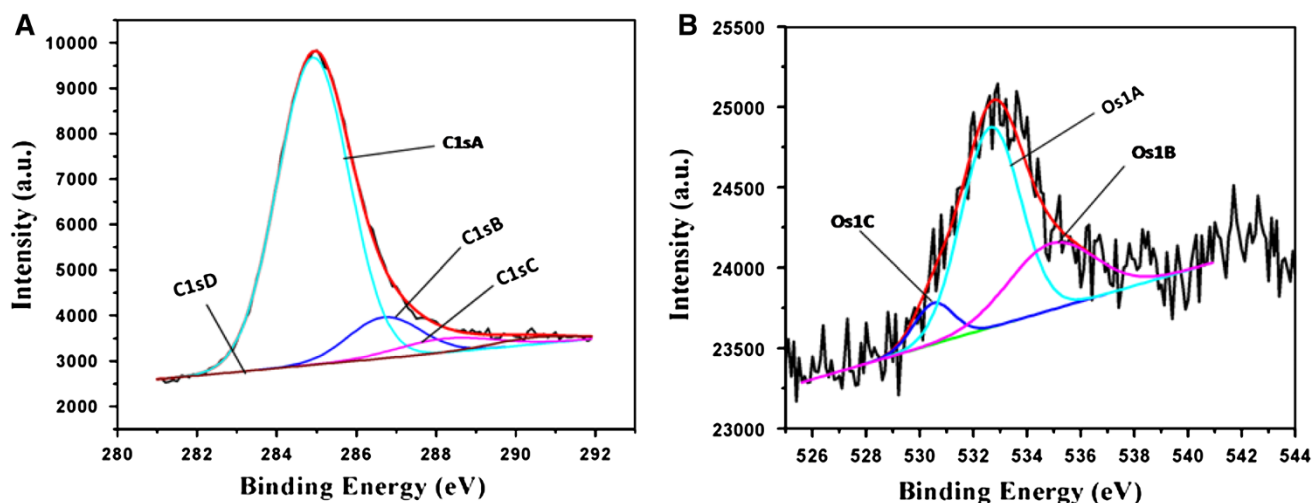


**Fig. 2** X-ray Photoelectron Spectroscopy spectra of semicoke (a) deconvoluted spectra of C1s region and (b) deconvoluted spectra of O1s region

**Table 1** Comparison of binding energies and atomic percentage of functional group

	Semicoke		MWCNTs	
	BE (eV)	Atomic (%)	BE (eV)	Atomic (%)
C–C $sp^2$ and $sp^3$	284.9	81.8	285.02	72.41
C–O, phenyl, ether	286.5	11.0	286.49	14.94
	532.64		532.67	
C=O, carbonyl, ketone and quinone	288.2	5.08	288.23	5.31
	530.5		530.69	
–COO, carboxyl, ester and anhydride	290	2.08	290.10	7.31
	534.89		532.15	
Total		100		1,000

tar pitch and semicoke are characterized by FT-IR, which is sensitive to the presence of specific functional groups in the materials. Figure 3 shows FT-IR spectra of coal tar

pitch and semicoke derived from coal tar pitch. In the case of coal tar pitch, peak in the region  $3,500\text{--}3,700\text{ cm}^{-1}$  is of NH stretching or OH stretching mode of water because

when a small amount of pitch powder is mixed with KBr it does not show the hydrogen-bonded NH groups but shows the strong OH peak.

The peak observed between the regions  $3,000\text{--}3,100\text{ cm}^{-1}$  is of aromatic C–H stretching mode. On the other hand, peaks in the region between  $2,800\text{--}3,000\text{ cm}^{-1}$  correspond to aliphatic hydrogen between  $-\text{CH}_2-$  and  $-\text{CH}_3-$  structure. The sharp peak around  $1,385\text{ cm}^{-1}$  is of  $-\text{CH}_3$  of aliphatic structure. The peak around  $1,630\text{ cm}^{-1}$  is of C=O vibration bond. The peak at  $1,090\text{ cm}^{-1}$  is of aryl-aryl/aryl-alkyl ether bond. In addition to these characteristic peaks, semicoke spectra have new peaks in the region between  $700$  and  $900\text{ cm}^{-1}$  related to aromatic, out-of-plane C–H bending with different degree of substitution (Guillen et al. 1995). The peaks of CH stretching mode is observed in between  $2,850$  and  $3,050\text{ cm}^{-1}$ . On the other hand, C=O peak shifted to lower wave number ( $1,606\text{ cm}^{-1}$ ) in case of the semicoke. These groups present on the MWCNTs and semicoke are responsible for interactions in the composites. Like graphite, MWCNTs are relatively non-reactive, except at the nanotubes' caps (pentagon–heptagon pair defects) which are more reactive due to the presence of dangling bonds. The reactivity of the side walls of the MWCNTs  $\pi$ -system can also be influenced by the tube curvature. This ultimately depends upon the processing of MWCNTs. Figure 3b, shows the FTIR spectra of MWCNTs. The peak at  $3,458\text{ cm}^{-1}$  is possibly of  $-\text{OH}$  from water hydroxyl and carboxyl groups. The peak around  $1,740\text{ cm}^{-1}$  is of C=O from ketonic, carboxylic, acid anhydride or ester groups. The peak at  $1,560\text{ cm}^{-1}$  of C=C bending vibration. The peaks between  $1,050$  and  $1,200\text{ cm}^{-1}$  are of C–O. The peak at around  $1,460\text{ cm}^{-1}$  is of C–H, CH,  $=\text{CH}_2$  and  $-\text{CH}_3$ . The FTIR

results are in agreement with results of XPS for semicoke and MWCNTs.

#### TGA of MWCNTs and semicoke

Figure 4 shows the TGA curve of coal tar pitch, semicoke and MWCNTs carried in nitrogen atmosphere. This will give quantitative idea of surface complex available on the material by mean of weight loss. In case of coal tar pitch, there is total 60 % weight loss because coal tar pitch contains the polyaromatic hydrocarbons called volatile matter. The weight loss is divided into two groups; sudden weight loss of 50 % between  $200$  and  $500\text{ }^\circ\text{C}$ , and from  $500$  to  $1,000\text{ }^\circ\text{C}$  region weight loss is nearly 10 %. However, in semicoke and MWCNTs, there is negligible weight loss up to  $500\text{ }^\circ\text{C}$ . Above  $500\text{ }^\circ\text{C}$ , weight loss of 8.7 % is due to the removal of volatile by-product. The total weight loss in MWCNTs up to  $1,000\text{ }^\circ\text{C}$  is 3.5 %. The weight loss is higher in case of semicoke as compared to MWCNTs due to the surface functional groups. The TGA observations are in agreement with XPS and FTIR studies which are responsible for making bonding in composites.

#### Thermo-mechanical properties of carbon composites

Figure 5 shows the bulk density of carbon composites heat treated at different temperatures with increasing MWCNTs content. In this study the self-sintering semicoke is used as reinforcement. The self-sintering semicoke consists of Q.I. content 94.7 %, T.I. content 97.8 % and  $\beta$  resin complex chemical fraction. The  $\beta$ -resin is the mathematical difference between T.I. and Q.I., which represents a large polynuclear molecular weight portion in pitch.

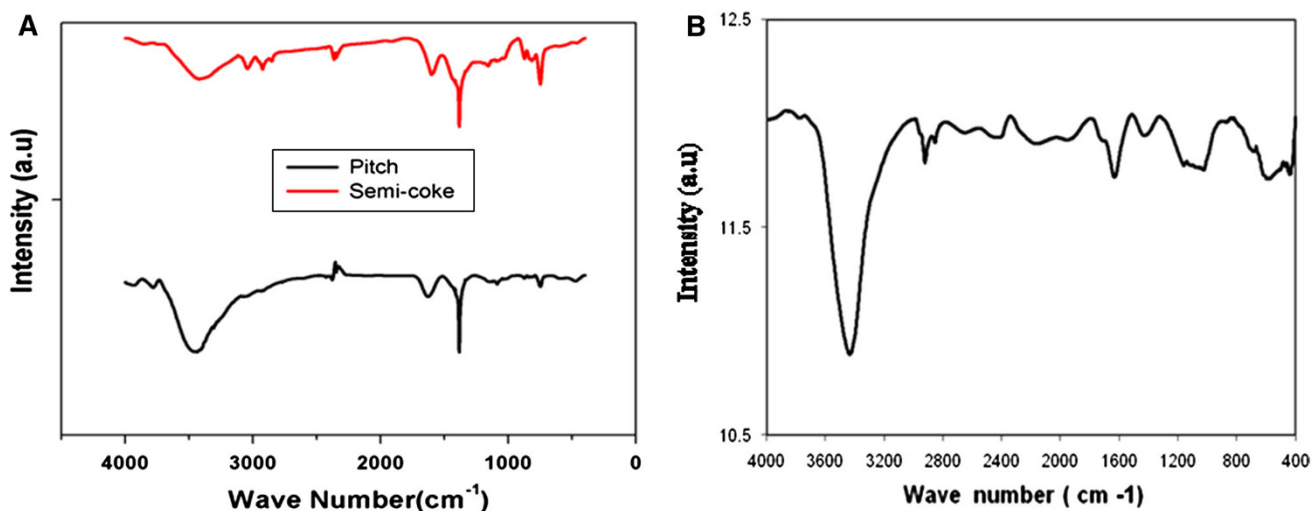


Fig. 3 FTIR spectra of a coal tar pitch and semicoke and b MWCNTs

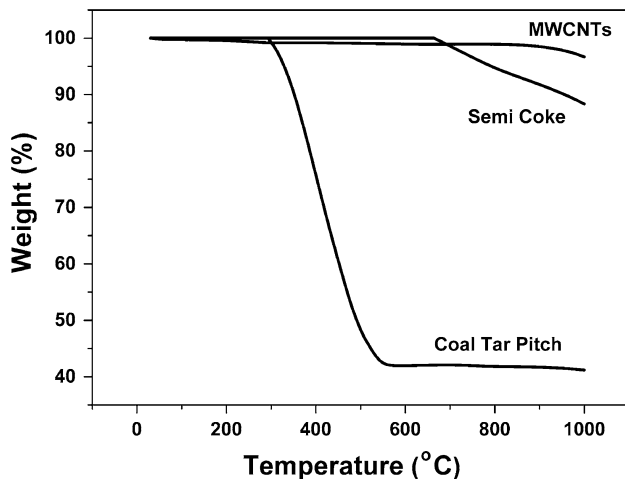


Fig. 4 TGA of coal tar pitch, semicoke and MWCNTs

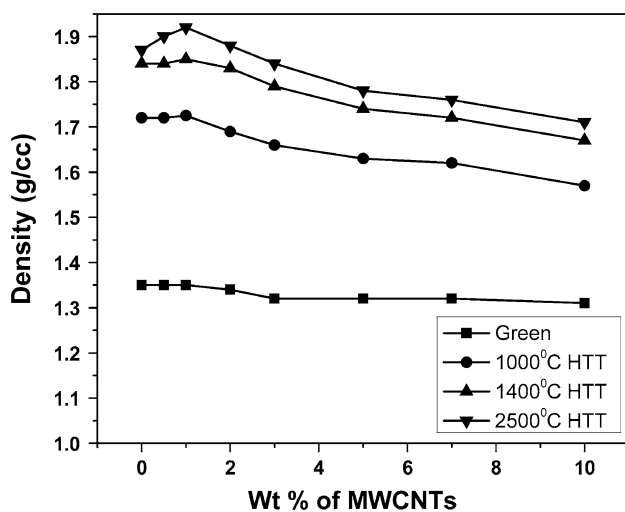
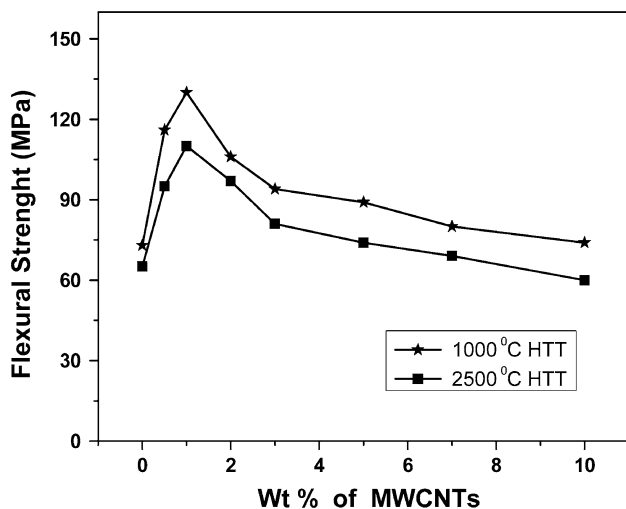


Fig. 5 Bulk density of carbon composites with increasing MWCNTs content and processing temperature

Initially, the bulk density of cold-pressed monolithic semicoke block as well as that of the MWCNTs-incorporated semicoke composite is almost in the same range. With increasing the nanotubes' contents, the bulk density of composite increases; but above 5 wt% of MWCNTs it slightly decreases. With increasing heat treatment temperature (carbonization and graphitization), the bulk density of the all composites increases continuously. During the heat treatment temperature,  $\beta$ -resin facilitates the bonding between the semicoke particles, semicoke particles and MWCNTs in the temperature range 300–500 °C, which contributes to bulk densification. However, in case of nanotubes-incorporated composites, bulk density increases up to certain content of nanotubes and above 1 % of MWCNTs, bulk density decreases continuously. During the heat treatment,  $\beta$  resin passes through fluid phase and it can wet with the carbon

nanotubes. As observed from the XPS, FTIR and TGA analysis,  $\beta$ -resin and MWCNTs consist of surface complexes in the form of oxygen containing functional groups, which are responsible for making interaction between them. The carbon nanotubes possess high specific surface area, which is much higher than  $\beta$ -resin surface area available within composites. Therefore, the  $\beta$ -resin content in the semicoke is not sufficient for wetting the higher content of MWCNTs, because semicoke itself as self-sintering material can also make interaction between the semicoke particles. This can result in poor densification of semicoke-based carbon composites at higher nanotubes contents and as a consequence decrease in bulk density with increasing the MWCNTs contents. The bulk density of carbon composites decreases from 1.72 to 1.57 g/cc (Fig. 5), same trend is persists with increasing the heat treatment temperature to 2,500 °C. The bulk density of carbon composites with 1 wt% of MWCNTs is 1.92 g/cc, which is higher as compared to that of without nanotubes semicoke based material 1.87 g/cc. To achieve this value of bulk density of C–C composites requires a number of densification cycles, expensive infrastructure, as well as time. This process of incorporating MWCNTs in semicoke-based composites is useful for the production of graphite electrode in single step.

Figure 6 shows the bending strength with increasing the MWCNTs content in composites. The bending strength of carbon composites heat treated at temperature 1,000 and 2,500 °C is illustrated in Fig. 6. In case of 1,000 °C heat treated (carbonized) carbon composites, bending strength increases with increasing nanotube content up to 1.0 wt%. Thereafter bending strength continuously decreases with increasing the MWCNTs content. The bending strength increases from 73 to 130 MPa at 1.0 wt% of MWCNTs and with further increasing the MWCNTs to 2 wt%, bending strength decreases to 100 MPa. The maximum decreases in strength at higher content of MWCNTs at 10 wt% and value of strength is equivalent to the value of 0 wt% of MWCNTs-based composites. This is due to high surface area of MWCNTs as compared to self-sintering semicoke. The minimal amount can accommodate effectively in the composites. The minimal amount of carbon nanotubes can homogeneously distribute in composite, which can increase the bonding force between self-sintering coke and carbon nanotubes. In these composites, the  $\beta$ -resin can facilitate the bonding of semicoke particles and carbon nanotubes. The  $\beta$ -resin passes through the fluid stage at temperatures between 300 and 500 °C and can wet carbon nanotubes. But due to the limited content of  $\beta$ -resin, it cannot wet higher content of carbon nanotubes as well as the problem of dispersion of nanotubes. It is also evident from the SEM figure that the carbon nanotubes bonded well with semicoke-derived carbon, and the diameter of the



**Fig. 6** Flexural Strength of carbon composites with increasing MWCNTs content and processing temperature

nanotubes is much higher than that of original nanotubes (Fig. 7).

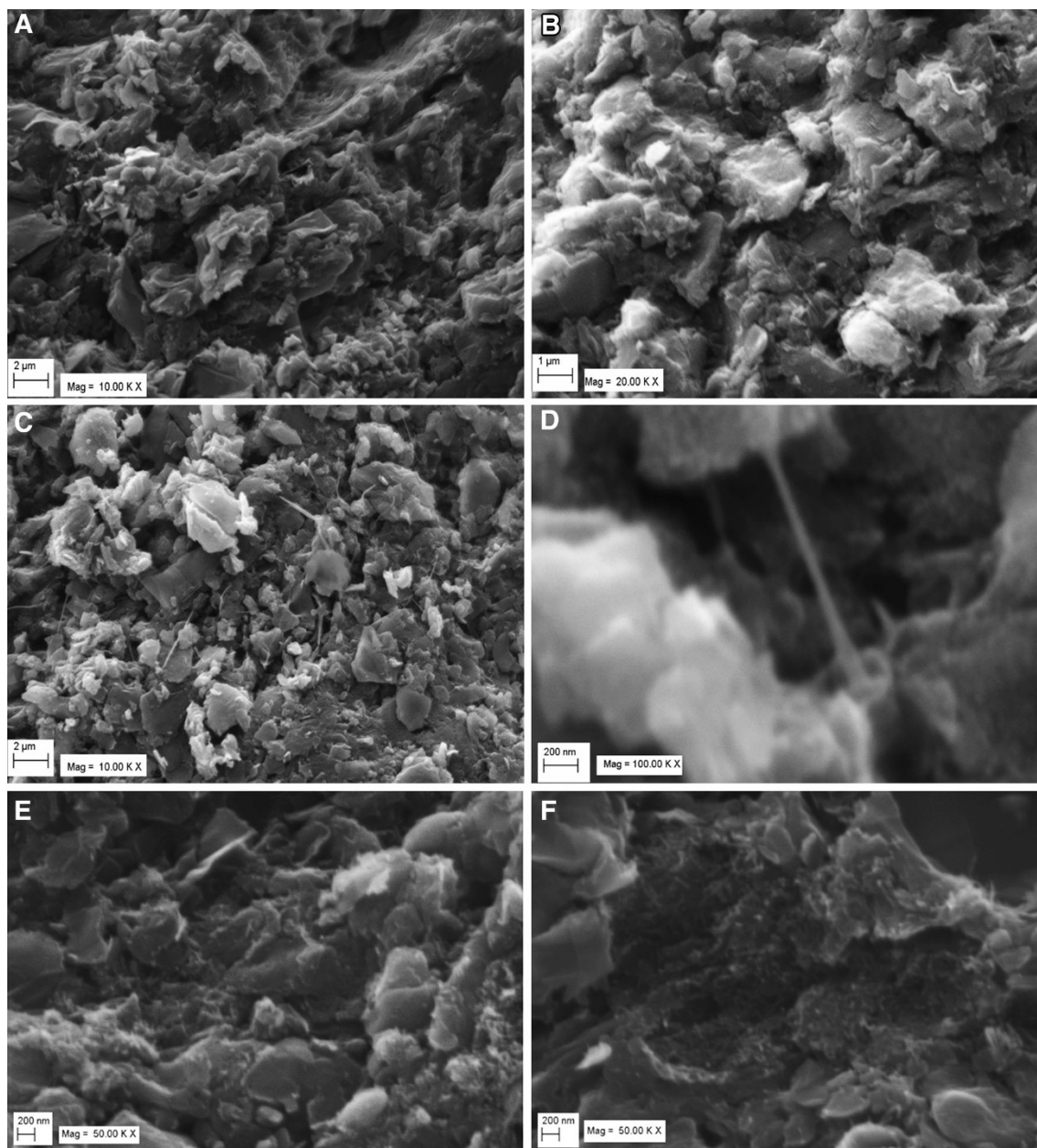
After graphitization, bending strength decreases in all the cases. The extent of decreases is higher in case 1.0 wt% MWCNTs-incorporated composites. This might be due to the fact that MWCNTs promote graphitization in carbon composites because carbon atom or graphene layer can grow in an orderly manner along MWCNTs axis in well bonded and dispersed nanotubes in the composites. The maximum value of strength is 110 MPa of 1 wt% MWCNTs-based composites, but above 1 wt% MWCNTs in carbon composites, strength continuously decreases. This can be due to the agglomeration, poor dispersion and lack of bonding. The higher content of MWCNTs obstructs the alignment of carbon atom due to the poor bonding and agglomeration of carbon nanotubes. This leads to disordering of carbon atom in carbon composites with higher content of carbon nanotubes. The increase in disordering of carbon atoms leads to decrease in electrical and thermal conductivity. The flexural strength is 110 MPa maximum achieved with 1 wt% MWCNTs in this study. However, in earlier reported data in literature, it is found that maximum flexural strength 67 MPa of mesophase pitch-based carbon composites with 20 wt% of MWCNTs (Song et al. 2007), 78.6 MPa of oxidized mesophase pitch based carbon composites with 5 wt% of MWCNTs (Song et al. 2008), 63 MPa of MCMB based carbon composites with 10 wt% MWCNTs (Moulder et al. 1992). This study shows that lower content of well dispersed CNTs in matrix can be useful for achieving the higher value of flexural strength.

Figure 7 shows SEM micrographs of 1,000 and 2,500 °C heat treated carbon composites. Figure 7a, b, SEM micrograph of carbon composites with 0 wt% of MWCNTs (1,000 and 2,500 °C heat treated), in which the

carbon derived by semicoke particles are densely packed due to its self sintering properties. In this study semicoke derived from coal tar pitch initially ball milled to get fine powder. However, in case of 1 wt% MWCNTs based carbon composites heat treated at 2,500 °C, MWCNTs are uniformly distributed in the semicoke derived carbon with dense packing (Fig. 7c). Figure 7d shows the MWCNTs are well bonded between the carbon matrix and MWCNTs is completely covered by carbon and as a consequence increases in the diameter of nanotubes. The bonding force between MWCNTs and carbon can reduce the sliding, hence it results into the improved bending strength of carbon composites. At higher content of MWCNTs (3 and 10 wt%) agglomeration of nanotubes resulted into the degradation of the properties of carbon composites on 2,500 °C heat treated composites (Fig. 7e, f). The MWCNTs are agglomerated not visible because the nanotube diameter is in the range of 25–30 nm only (Fig. 8).

Figure 9 shows the variation in electrical conductivity of carbon composites with increasing the MWCNTs content. The electrical conductivity initially of carbon derived from semicoke heat treated at 1,000 °C is 263 S/cm and with increasing the MWCNTs content it increases to 280 S/cm at MWCNTs content 1 wt% in carbon composites. With increasing the MWCNTs content electrical conductivity is continuously decreases. However, maximum electrical conductivity is 395 S/cm at 1.0 wt% of MWCNTs in case of 1,400 °C heat treated carbon composites. Thereafter similar trend registers with increasing the MWCNTs content as with 1,000 °C heat treated composites. However, at 2,500 °C heat treated composites, electrical conductivity increases in all the cases this is due to the increase in degree of graphitization due to the ordering of graphitic layer along the axis of MWCNTs. The increase in electrical conductivity is due to the increase in conduction path of electron which is directly related to structure of reinforcing material. This is verified by XRD and Raman spectroscopy studies.

Figure 10 shows the thermal conductivity and interlayer spacing of carbon-composites with increasing the nanotube content. Without nanotube in semicoke derived carbon block heat treated at 2,500 °C, thermal conductivity is 45 W/m K. However, thermal conductivity increases to 60 W/m K at 1 wt% MWCNTs of carbon composites. In the composites, carbon atoms or graphene layer aligned parallel to CNTs axis and as a result decreases in the interlayer spacing and increases in the crystalline parameters. This is due to the anisotropic thermal expansion of MWCNTs and carbon derived from semicoke, during heat treatment mechanical stresses exerting at MWCNT/carbon interface and accelerates ordering of the graphene layer. If compared the two curves of interlayer spacing and the



**Fig. 7** SEM micrographs of **a** 0 % MWCNTs carbon-composites heat treated at 1,000 °C, **b** 0 % MWCNTs carbon-composites heat treated at 2,500 °C, **c** and **d** 1 % MWCNTs carbon-composites heat

treated at 2,500 °C, **e** 3 % MWCNTs carbon-nano composites heat treated at 2,500 °C and **f** 10 % MWCNTs carbon-composites heat treated at 2,500 °C

thermal conductivity, it is found that, both are progresses with opposite to each other. Figure 11 shows the XRD spectra of 2,500 °C heat treated carbon composites. Initially in case of 2,500 °C heat treated composite the interlayer spacing without MWCNTs is 0.3367 nm and in case of composites with 1 wt% of MWCNTs, interlayer spacing decreases to 0.3355 nm. However, with increasing the nanotubes content, the interlayer spacing of carbon composites increases continuously. The interlayer spacing of carbon composites is 0.3358, 0.3365 nm for 2 and

5 wt% of MWCNTs respectively. With increasing nanotubes content in the carbon composites, interlayer spacing increases is due to the higher content of MWCNTs obstructs the alignment of carbon atom due to the poor bonding and agglomeration of carbon nanotubes. This has the negative effect on the thermal conductivity of carbon composites. The thermal conductivity of the composites decreases with increasing MWCNTs content and minimum thermal conductivity 27 W/m K at 10 wt% of MWCNTs. It is implicated that higher content of MWCNTs seems to



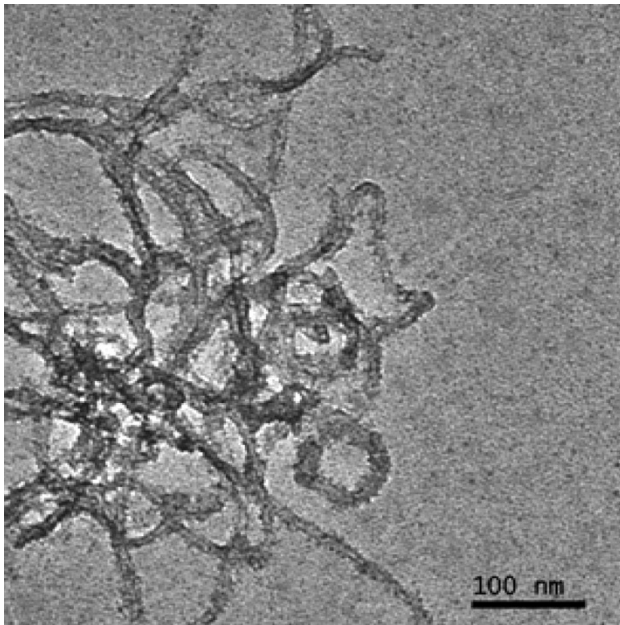


Fig. 8 TEM micrograph of MWCNTs

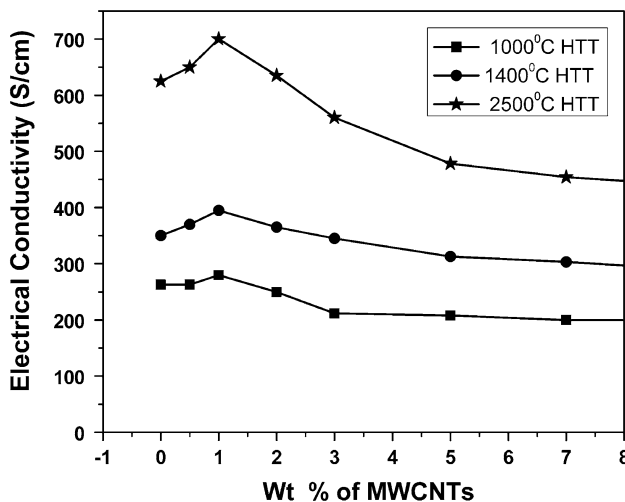


Fig. 9 Electrical Conductivity of carbon composites with increasing MWCNTs content and processing temperature

play thermal/electrical barrier in carbon matrix due to the increase in MWCNT to MWCNT interface and grain boundaries in composites. These grain boundaries are increases by the mixing of two different dissimilar particles because MWCNTs have nano-meter in size and self-sintering coke have size in micron, so non homogeneous mixture as formed.

The Raman spectra of MWCNTs and MWCNTs based carbon composites shows mainly three Raman bands at  $\sim 1,355\text{ cm}^{-1}$  (D band),  $\sim 1,585\text{ cm}^{-1}$  (G band), and  $\sim 2,710\text{ cm}^{-1}$  (second order band). The  $I(D)/I(G)$  ratio [where  $I(D)$  and  $I(G)$  are the D-band and G-band Raman intensities, respectively] is commonly used to measure the

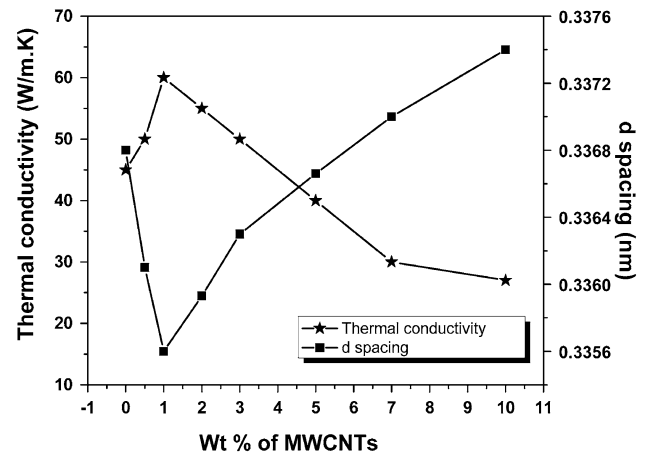


Fig. 10 Thermal conductivity and interlayer spacing of carbon composites with increasing MWCNTs content and processing temperature

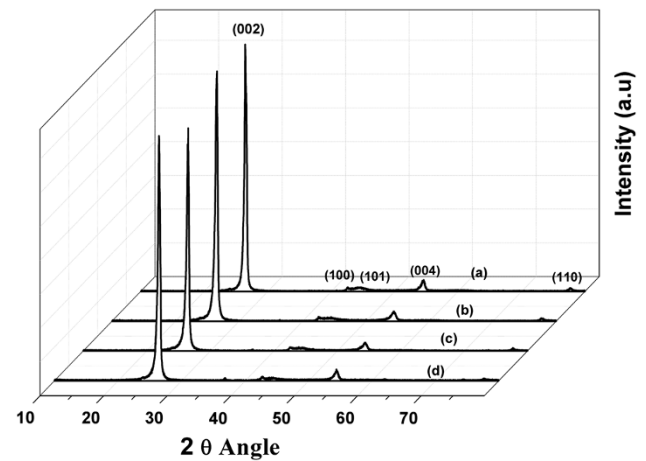
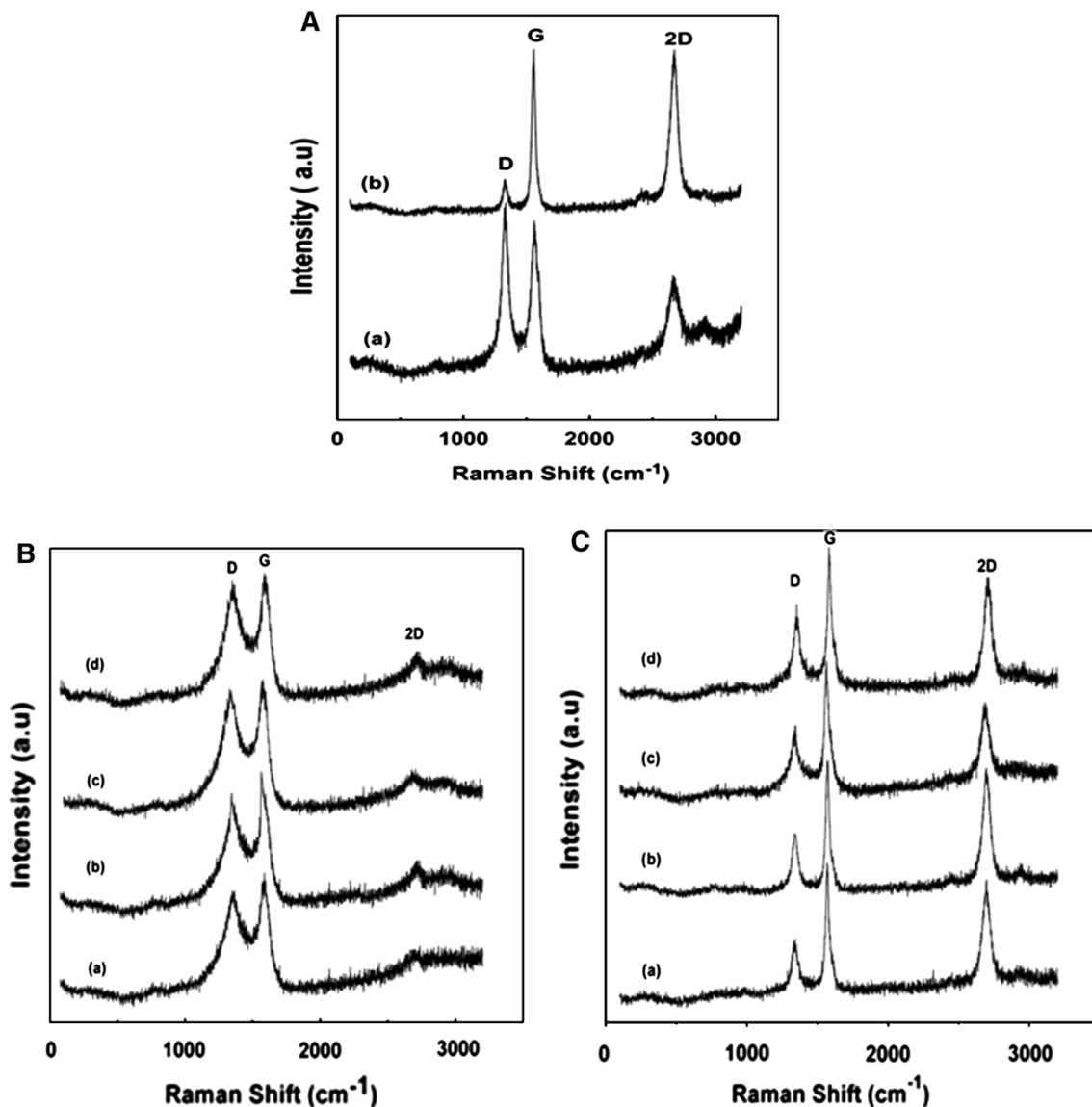


Fig. 11 XRD spectra of carbon-composites heat treated at 2,500 °C, curve (a) 0 % MWCNTs, curve (b) 1 % MWCNTs, curve (c) 2 % MWCNTs and curve (d) 5 % MWCNTs

imperfection in the graphene lattice, as it corresponds to the relative population of  $sp^3$ -hybridization carbon atoms and it is also an indicative of the abundance of edge atoms (Dhakate et al. 2011). It is used to estimate the density of defects in the CNT structure and the fraction of in-plane crystallite in the graphite structure (Tuinstra and Koenig 1970; McCulloch et al. 1994).

Figure 12a shows the Raman spectra of as received MWCNTs and 2,500 °C heat treated MWCNTs. In case of as such MWCNTs, D-band intensity is higher as compared to G-band, on the other hand in case of heat treated 2,500 °C, G-band intensity is higher as compared to D-band. This is due to the perfection in CNTs structure on heat treatment at higher temperature. This is measured by comparing the  $I(D)/I(G)$  ratios.

In case of as such MWCNTs,  $I(D)/I(G)$  ratio is 1.1031 and 2,500 °C heated treated MWCNTs is reduced to



**Fig. 12** Raman spectra **A** As such MWCNTs curve (a) and 2,500 °C heat treated MWCNTs curve (b), **B** carbon-composites heat treated at 1,000 °C, curve (a), (b), (c) and (d) 0, 1, 2, and 5 % MWCNTs

respectively, **C** carbon-composites heat treated at 2,500 °C, curve (a), (b), (c) and (d) 0, 1, 2, and 5 % MWCNTs

0.2514. Figure 12b, c) shows the Raman spectra of 1,000 and 2,500 °C carbon composites. In case 1,000 and 2,500 °C heat treated carbon composites the  $I(D)/I(G)$  ratio varies with MWCNTs content. Initially without MWCNTs based composite  $I(D)/I(G)$  ratio of 1,000 °C heat treated material is 0.8779 and that of 2,500 °C is 0.5232. The decrease in  $I(D)/I(G)$  ratio is due to the graphitization of carbonaceous semicoke based materials. On addition of different content of MWCNTs, The minimum value of  $I(D)/I(G)$  ratio in case of 1 wt% based carbon composites, 1,000 °C heat treated composites it is 0.8670 and that of 2,500 °C is 0.4981 and increasing the MWCNTs content to 2 wt% the value of  $I(D)/I(G)$  increases in both type of

composites i.e., 0.9390 and 0.5892 of heat treated 1,000 and 2,500 °C. However, further increasing the MWCNTs content to 5 wt%,  $I(D)/I(G)$  ratio increases in both type of composites i.e., 0.9498 and 0.6686 of heat treated 1,000 and 2,500 °C. This shows that the above 1 wt% of MWCNTs can obstruct graphitization of carbon composites. But one interesting fact that as such heat treated MWCNTs is well graphitized and  $(ID)/(IG)$  ratio 0.2514 as compared 5 wt% MWCNTs based composites  $(ID)/(IG)$  ratio 0.6686. This shows that higher content of MWCNTs in composites restrict the degree of graphitization. These results are in the agreement with also XRD measurements. It is found that, the trend of XRD data is similar to Raman studies.

## Conclusions

The carbon composites are developed using semicoke and MWCNTs with different weight contents. The XPS results show the MWCNTs and semi-coke possesses different amount of surface complexes. The XPS and FTIR results are in compliment with each other. It is found that in the semi-coke based composites  $\geq 1$  wt% of nanotubes have adverse effects on the overall properties. The maximum bulk density, bending strength, electrical and thermal conductivity achieved with 1 wt% of MWCNTs based carbon composites. The results of Raman spectroscopy studies and X-ray diffraction are in agreement with mechanical, thermal and electrical properties of carbon composites. The flexural strength of carbonized composites is increases by 78 % and that of graphitized by 69 % at 1 wt% of MWCNTs. The value of flexural strength is three times higher than the value of conventional graphite. The electrical and thermal conductivity increases by 12 and 33 % respectively. This study clearly brings out that few percentage of nanotubes well dispersed in semi-coke is suitable for influencing the properties of carbon composites.

Further, if the electrical and thermal conductivity of semicoke based composites tailored then it may be used is many applications.

**Acknowledgments** Authors are highly grateful to Director, CSIR-NPL, for his kind permission to publish the results. Also thanks Mr. Jai Tawale and Mr. Sood, for providing SEM characterization facilities. One of the authors (Rajeev Kumar) would like to thanks CSIR for SRF fellowship.

**Open Access** This article is distributed under the terms of the Creative Commons Attribution License which permits any use, distribution, and reproduction in any medium, provided the original author(s) and the source are credited.

## References

- Ajayan PM, Stephan O, Colliex C, Trauth D (1994) Aligned carbon nanotubes arrays formed by cutting a polymer resin-nanotube composite. *Science* 265:1212
- Aly-Hasan MS, Hatta H, Wakayama S, Watanabe M, Miyagawa K (2003) Comparison of 2D and 3D carbon-carbon composites with respect to damage and fracture resistance. *Carbon* 41:1069
- Bhatia G, Aggarwal RK, Punjabi N, Bahl OP (1994) Formation of mesophase spherules in low-QI coal-tar pitches and development of monolithic carbons therefrom. *J Mats Sci* 29:4757
- Blanco C, Santamaria R, Bermejo J, Menendez R (2000) Pitch-based carbon composites with granular reinforcements for frictional application. *Carbon* 38:1043
- Dhakate SR, Chauhan N, Sharma S, Tawale J, Singh S, Sahare PD, Mathur RB (2011) A new approach to produce single and double layer graphene from re-exfoliation of expanded graphite. *Carbon* 49:1946
- Dresselhaus M, Avouris P (2001) Carbon nanotubes: synthesis, structure properties and applications. Springer, Berlin
- Fitzer E (1987) The future of carbon-carbon composites. *Carbon* 25:163
- Gao Y, Song H, Chen X (2002) Preparation of C/C composite using mesocarbon microbeads as matrix. *J Mater Sci Lett* 21:1043
- Gao X, Liu L, Guo Q, Shi J, Zhai G (2005) Fabrication and mechanical/conductive properties of multiwalled carbon nanotubes reinforced carbon matrix composite. *Mats Letts* 59:3062
- Guillen MD, Iglesias MJ, Dominguez A, Blanco CG (1995) Fourier transforms infrared study of coal tar pitches. *Fuel* 74:1595
- Iijima S (1991) Helical microtubes of graphitic carbon. *Nature* 354:56
- Li HJ (2001) Carbon-carbon composites. *New Carbon Mater* 16:79
- Mantell CL (1968) Carbon and graphite hand book. Wiley Interscience, New York
- McCulloch DG, Praver S, Hoffman A (1994) Structural investigation of xenon-ion-beam-irradiated glassy carbon. *Phys Rev B* 50:5905
- Moulder JF, Sticle WF, Sobol PE, Bombe KD (1992) Handbook of X-ray photoelectron spectroscopy. Perkin-Elmer Co, Eden Prairie
- Ning JW, Zhang JJ, Pan YB, Guo JK (2003) Fabrication and mechanical properties of SiO<sub>2</sub> matrix composites reinforced by carbon nanotubes. *Mater Sci Eng A-Struct Mater Prop Microstruct Process* 357:392
- Peigney A, Laurent CH, Flahaut E, Rousset A (2000) Carbon nanotube in novel ceramic matrix composites. *Ceram Int* 26:677
- Qiu HP, Song YZ, Liu L, Zhai G, Shiet J (2003) Thermal conductivity and microstructure of Ti-doped graphite. *Carbon* 41:973
- Schmidt J, Moergenthaler KD, Brehler KP, Arndt J (1998) High strength graphite for carbon piston application. *Carbon* 36:1079
- Song YZ, Zhai GT, Li GS, Shij L, Guo QG, Liu L (2004) Carbon/graphite seal materials prepared from mesocarbon microbeads. *Carbon* 42:1427
- Song Y, Zhai G, Shi J, Guo Q, Liu L (2007) Carbon nanotubes: carbon composite with matrix derived from oxidized mesophase pitch. *J Mater Sci* 42:9498
- Song Y, Li S, Y. Zhai G, Shi J, Guo Q, Liu L, Xu Z, Wang J (2008) Mechanical and physical properties of MWCNT/Carbon composites with matrix derived from mesocarbon microbeads. *Carbon* 46:1091
- Thomas CR (ed) (1993) Essentials of carbon-carbon composites. Royal Society of Chemistry, London
- Titantah T, Lamoen D (2005) sp<sup>3</sup>/sp<sup>2</sup> Characterization of carbon materials from first-principles calculations: X-ray photoelectron versus high energy electron energy-loss spectroscopy techniques. *Carbon* 43:1311
- Tuinstra F, Koenig JL (1970) Raman spectrum of graphite. *J Chem Phys* 53:1126
- Wang YG, Korai Y, Mochida I (1999) Carbon disc of high density and strength prepared from synthetic pitch-derived mesocarbon microbeads. *Carbon* 37:1049
- Yu M, Files BS, Arepalli S, Ruoff RS (2000a) Tensile loading of ropes of single wall carbon nanotubes and their mechanical properties. *Phys Rev Lett* 84:5552
- Yu M, Lourie O, Dyer MJ, Moloni K, Kelly TF, Ruoff RS (2000b) Strength and breaking mechanism of multiwalled carbon nanotubes under tensile load. *Science* 287:637